J Eur Ceram Soc (2016), http://dx.doi.org/10.1016/j.jeurceramsoc.2016.03.018

Dielectric ceramic with stable relative permittivity and low loss from -60 to 300 ºC: a potential high temperature capacitor material

Saeed Ullah Jan, Aurang Zeb and Steven J. Milne

Institute for Materials Research, School of Chemical and Process Engineering, University of Leeds, Leeds, LS2 9JT, UK

Saeed Ullah Jan janicup@gmail.com

Aurang Zeb zebicp@gmail.com

Aurang Zeb <zebicp@gmail.com>s.j.milne@leeds.ac.uk

J Eur Ceram Soc (2016), http://dx.doi.org/10.1016/j.jeurceramsoc.2016.03.018

Dielectric ceramic with stable relative permittivity and low loss from -60 to 300 ºC: a potential high temperature capacitor material

Saeed Ullah Jan, Aurang Zeb and Steven J. Milne

Institute for Materials Research, School of Chemical and Process Engineering, University of Leeds, Leeds, LS2 9JT, UKA

Abstract

A new dielectric is described that meets the industry-standard lower limiting temperature of stable performance, -55 °C whilst extending the upper limit to 300 °C, with low dielectric loss, as required for the developing high-temperature electronics sector. The combined substitution of Sr and Bi ions on A sites, and Mg and Zr ions on B sites of the ABO_3 perovskite solid solution $(1-x)Ba_{0.6}Sr_{0.4}Zr_{0.2}Ti_{0.8}O_3$-$xBi(Mg_{0.5}Ti_{0.5})O_3$, flattens the ε_r -T response. At composition x = 0.2 the $\varepsilon_{r\ max}$ temperature , and the associated tan δ dispersion peak, are each displaced to low temperatures such that a very favourable combination of low dielectric loss, tanδ < 0.015, from -60 to 310 °C and stable ε_r, ~ 500 ± 15 % from -70 to 300 °C (1 kHz data) is demonstrated. The x = 0.2 material achieves stable ε_r and low loss over the technologically important target temperature range, -55 to 300 °C.

Introduction

There is growing interest in developing high-temperature, high relative permittivity dielectric ceramics (lead-free) for Class II capacitors in electronic systems that can operate at elevated temperatures, well beyond 200 ºC [1, 2]. Conventional barium titanate ferroelectric based capacitors retain stable relative permittivity, ε_r, within ±15 % from a lower operating temperature limit of -55 ºC to upper temperatures of 125 – 175 ºC (as specified by the Electronic Industries Alliance for X7R – X9R type Class II capacitor materials). In recent years, alternative perovskite ceramics, based on relaxor dielectrics have shown promising ε_r temperature-stability to much higher temperatures than X7R – X9R.

The ε_r–T response of these temperature-stable relaxors differs substantially from that of a normal relaxor, such as $Pb(Mg_{1/3}Nb_{2/3})O_3$, in that the normal broad ε_r(T) relaxor peak (at temperature T_m) is supressed, to give a plateau with only a slight variation in ε_r (within ± 15 %) across a broad temperature range. The materials are compositionally modified perovskites, ABO_3 which incorporate Bi^{3+} on A-sites [3- 20] as reviewed in reference [21], for example $(1–x)BaTiO_3 – xBi(Mg_{0.5}Ti_{0.5})O_3$ solid solutions [3-7]. The level of stability in ε_r(T) for $(1–x)BaTiO_3 – xBi(Mg_{0.5}Ti_{0.5})O_3$ becomes more pronounced with additional Ca^{2+} substitution**,** giving ε_r values ~ 1000 ± 15 % (1 kHz) from 80 – 500 °C [3].

One possible reason for the change from normal to temperature-stable relaxor behaviour is that the increases in size and coupling of polar nanoregions on cooling below the Burn's temperature, T_B that create a distinctive, broad ε_r-T peak in a normal relaxor are inhibited in heavily substituted perovskite relaxors which invariably involve Bi ion substitution. However the mechanisms underpinng temperature-stable relaxors are uncertain. In most reports of novel high temperature dielectrics, the lower temperature limit of stable ε_r(T) is generally above room temperature: these materials fail to accomplish the Electrical Industries Alliance (EIA) 'X' specification of stability in ε_r to -55 °C [21]. However, there are a few exceptions, for example,

$(Ba,Ca)TiO_3 – Bi(Mg_{0.5}Ti_{0.5})O_3 – NaNbO_3$ [BCT – BMT – NN], with $\varepsilon_r \sim 600 \pm 15$ % from ~ -70 °C to 300 °C and $\tan\delta \leq 0.02$ from -60 °C to 300 °C [1, 8]. Other examples include: $(1–x)[0.94Na_{0.5}Bi_{0.5}TiO_3 – 0.06BaTiO_3] – xCaZrO_3$, with $\varepsilon_r \sim 470 \pm 15$ % from ~ -40 °C to 450 °C, but in this case the estimated range of $\tan\delta \leq 0.02$ (as required for many devices) is restricted to the temperature range +50 °C to 200 °C (estimated) [2, 20]; $(1–x)[0.82(0.94Na_{0.5}Bi_{0.5}TiO_3 – 0.06BaTiO_3) – 0.18K_{0.5}Na_{0.5}NbO_3] – 0.2CaZrO_3$, with $\varepsilon_r \sim 400 \pm 15$ % from ~ -30 °C to 400 °C, and $\tan\delta \leq 0.02$ from 20 °C to 180 °C (estimated) [20]; and the system $BaTiO_3 – Na_{0.5}Bi_{0.5}TiO_3 – Nb_2O_5$, with $\varepsilon_r \sim 2404 \pm 13$ % from ~ -55 °C to 375 °C, but only room-temperature tanδ data were reported [19].

Here we have examine the effects of Sr (A-site) and Zr (B-site) modifications to a $BaTiO_3$ end-member: focussing on the composition, $Ba_{0.6}Sr_{0.4}Zr_{0.2}Ti_{0.8}O_3$. These substituents are known to reduce the Curie point temperature in the parent $BaTiO_3$ ceramic. Further compositional modifications were achieved by exploring solid solutions along the compositional join $(1-x)Ba_{0.6}Sr_{0.4}Zr_{0.2}Ti_{0.8}O_3- xBi(Mg_{0.5}Ti_{0.5})O_3$, creating additional Bi^{3+} ion substitution on A-sites and Mg^{2+} on B sites.

A ±15 % stability in ε_r satisfying the target -55 ºC to 300 °C temperature range, along with very low dielectric loss over the same temperature range is demonstrated in the new solid solution at composition x = 0.2. These properties are consistent with 'X_ R' characteristics according to the EIA specifications, but permittivity is lower than for the X7R family. The shift in ε_r peak temperature, T_m to well below -55 °C in the x = 0.2 sample is of critical importance: it allows a flat ε_r response to a temperature ≤ -55 °C and simultaneously shifts the relaxor-like tanδ dispersion peak to even lower temperatures, thereby preventing tan δ increasing to > 0.015 at -55 °C.

Experimental Procedure

Ceramics samples of $(1–x)Ba_{0.6}Sr_{0.4}Zr_{0.2}Ti_{0.8}O_3 – xBi(Mg_{0.5}Ti_{0.5})O_3$, x = 0 – 0.7, abbreviated BSZT – BMT, were prepared by a mixed oxide route from: $BaCO_3$ (≥ 99% purity, Alpha Aesar, Ward Hill, MA); Bi_2O_3 (Sigma-Aldrich, 99.9% purity, St. Louis, MO); TiO_2 (99.9%, (Sigma-Aldrich, 99.9% purity, St. Louis, MO); ZrO_2 (99.9%, (Sigma-Aldrich, 99.9% purity, St. Louis, MO); $SrCO_3$ (99.9%, Sigma Aldrich St. Louis, MO); MgO (99.9%; Alpha Aesar, Ward Hill, MA). The starting reagents were dried in an oven at 200 ºC and cooled to room temperature in a desiccator, prior to weighing. The powders were ball milled overnight, dried and sieved through 300-μm nylon mesh. The powders were calcined at 850 ºC for 4 h at heating and cooling rates of 300 ºC/h, sieved, and re-milled overnight after adding 1 % binder (Ciba Glascol HA4; Ciba Speciality Chemicals, Bradford, UK). The powders were uniaxially compacted at 75 MPa into pellets, 10 mm diameter and ~ 2 mm thickness in a stainless steel die, followed by cold isostatic pressing at 200 MPa. The pellets were embedded in calcined powder of the same batch in a closed alumina crucible, and sintered at 1150 ºC for 10 h, except for the x = 0 sample which was sintered at 1400 ºC for 4 h.

Phase formation was studied using X-ray powder diffraction (XRD, Bruker D8, Karlsruhe, Germany, Cu Kα ~ 1.5406 Å, scan speed 1º/min); powders for XRD were obtained by crushing sintered ceramic pellets. Lattice parameters were calculated from the unit cell d-spacings using a least square refinement method. The geometrical densities of the ceramic pellets were compared with theoretical density calculated from lattice parameters and assumed unit cell contents. For electrical testing, opposite surfaces of the sintered discs were ground and polished before applying silver paste (Agar Scientific, Stanstead, Essex, UK); samples were heated at 550 ºC for ~10-15 min to form the electrodes. Relative permittivity and loss tangent as a function of temperature were measured using an impedance analyzer (HP Agilent, 4192A Hewlett Packard Santa Clara, CA) in the temperature range 25 ºC – 400 ºC; low temperature measurements were recorded in the temperature range -70 – 30 ºC using the impedance analyser coupled to an environmental chamber

(TJR; Tenney Environmental-SPX, White deer, PA). The temperature range of 'stable' relative permittivity was calculated, according to the temperatures across which there was a stability within ±15% of a mid ε_r value. Polarization electric field, P-E, response was measured at room temperature using a LC precision analyser (Radiant Technologies Inc., Albuquerque, New Mexico).

Results and Discussion

Room temperature X-ray powder diffraction patterns of crushed sintered pellets of (1–x)BSZT – xBMT revealed a single-phase perovskite cubic pattern for all compositions: x = 0 – 0.5, Figure 1. An unidentified secondary phase appeared in sample compositions, x = 0.6 and 0.7. The cubic unit cell lattice parameter decreased linearly with increasing BMT content, for $x \geq 0.1$, as shown in Figure 2.

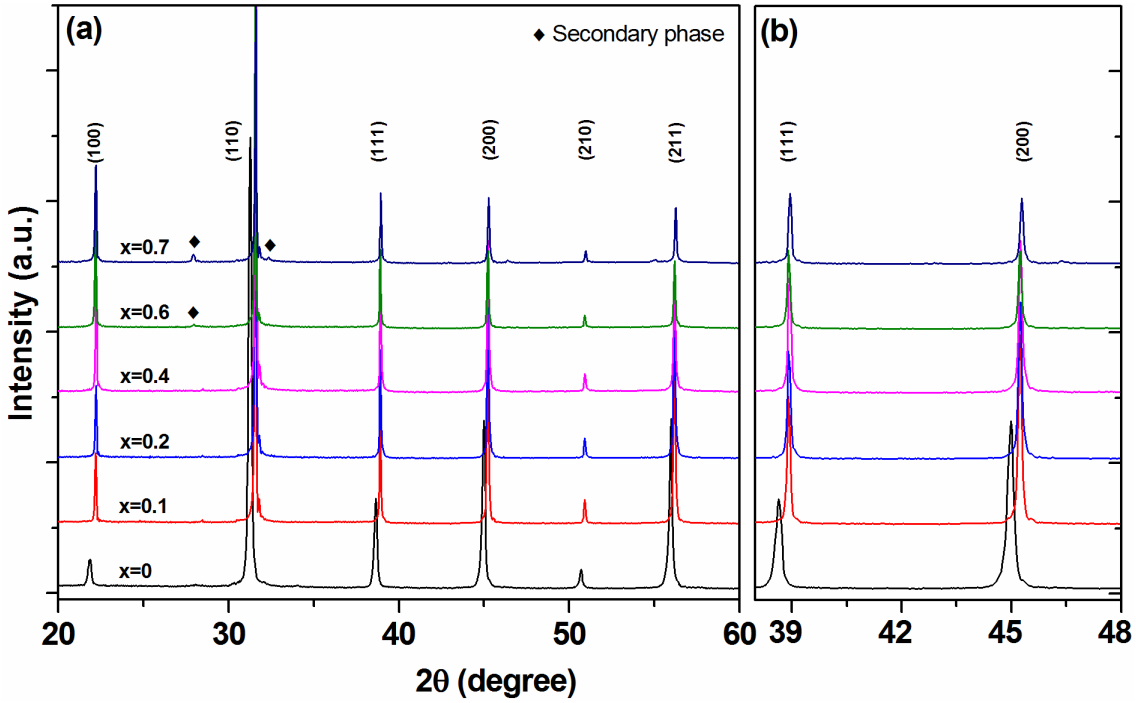

Figure 1. (a) X-ray powder diffraction patterns of crushed sintered pellets for (1-x)$Ba_{0.6}Sr_{0.4}Zr_{0.2}Ti_{0.8}O_3$ - x$Bi(Mg_{0.5}Ti_{0.5})O_3$: (b) expanded view of 111 and 002/200 peaks.

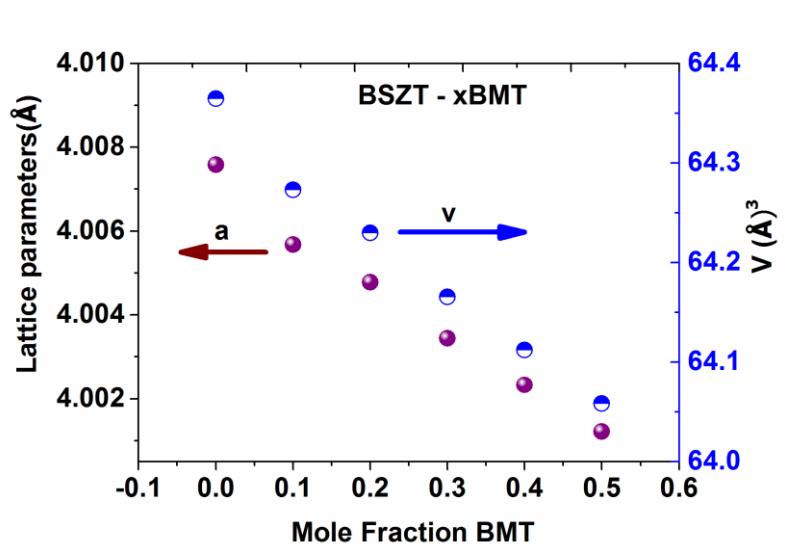

Figure 2. Variation of lattice parameter a and unit cell volume v as a function of x in (1-x)$Ba_{0.6}Sr_{0.4}Zr_{0.2}Ti_{0.8}O_3$ - x$Bi(Mg_{0.5}Ti_{0.5})O_3$.

Dielectric properties are summarised in Table 1 for all compositions studied. The temperature dependence of relative permittivity, ε_r, and dielectric loss tangent, tanδ, measured at various fixed frequencies, from -70 ºC to 400 ºC, is shown in Figure 3. The $\varepsilon_r(T)$ plot (at 1 kHz) for the x = 0 end-member, which is a Sr and Zr- modified $BaTiO_3$, inferred that a ε_r peak lay well below -70 ºC (i.e. below the temperature range of the environmental chamber), Figure 3(a). At composition x = 0.2, a broad maximum in the $\varepsilon_r(T)$ peak was evident, with T_m estimated $T_m \sim$ -20 °C (1 kHz), Figure 3(c).

Temperature-stable ε_r over wide temperature ranges was shown by compositions $0.1 \leq x \leq 0.7$. Of most interest, sample composition x = 0.2 maintained a stable $\varepsilon_r(T)$ response, $\varepsilon_r = 500 \pm 15$ % (1 kHz) across the temperature range, -70 to 300 °C, along with low dielectric loss, $\tan\delta \leq 0.015$ (1 kHz) for all temperatures from -60 to 310 °C.. Sample composition x = 0.3 displayed stable ε_r from -60 to 340 °C, but the lower temperature limit of low tanδ was only -10 °C. The characteristic relaxor dispersion peak in tanδ occurred $\geq$ 70 °C below T_m for each composition, x. In the case of composition x = 0.2, $T_m \sim$ -20 °C (1 kHz) and the tanδ peak (1 kHz) fell well below the minimum measurement temperature -70 °C. This allowed for a low value of tanδ, $\leq$ 0.015, down to -60 °C.

The limiting temperatures of the plateaux in ε_r shifted to higher temperatures for $x \geq 0.4$. Values of T_m control the lower limit of ± 15 % stability in ε_r in these materials (the lower limit occurs ~60-80 °C below T_m). Figure 4 illustrates the trend of increasing T_m and increasing peak ε_r values with increasing x. At x = 0.6 the $\varepsilon_{r\,mid}$ reached 1000 but the lower temperature limit rose to +50 °C.

The estimated values of dc resistivity were of the order of 10^9 Ω m at 300 ºC for x = 0.2 - 0.4. The RC values at 300 ºC increased from 3.7 s for x = 0.2 to 6.5 s for x = 0.4, Table 1. Above 300 ºC losses increased sharply which is attributed to increased conduction arising from lattice defects induced through volatilisation of bismuth oxide (similar phenomena are well documented

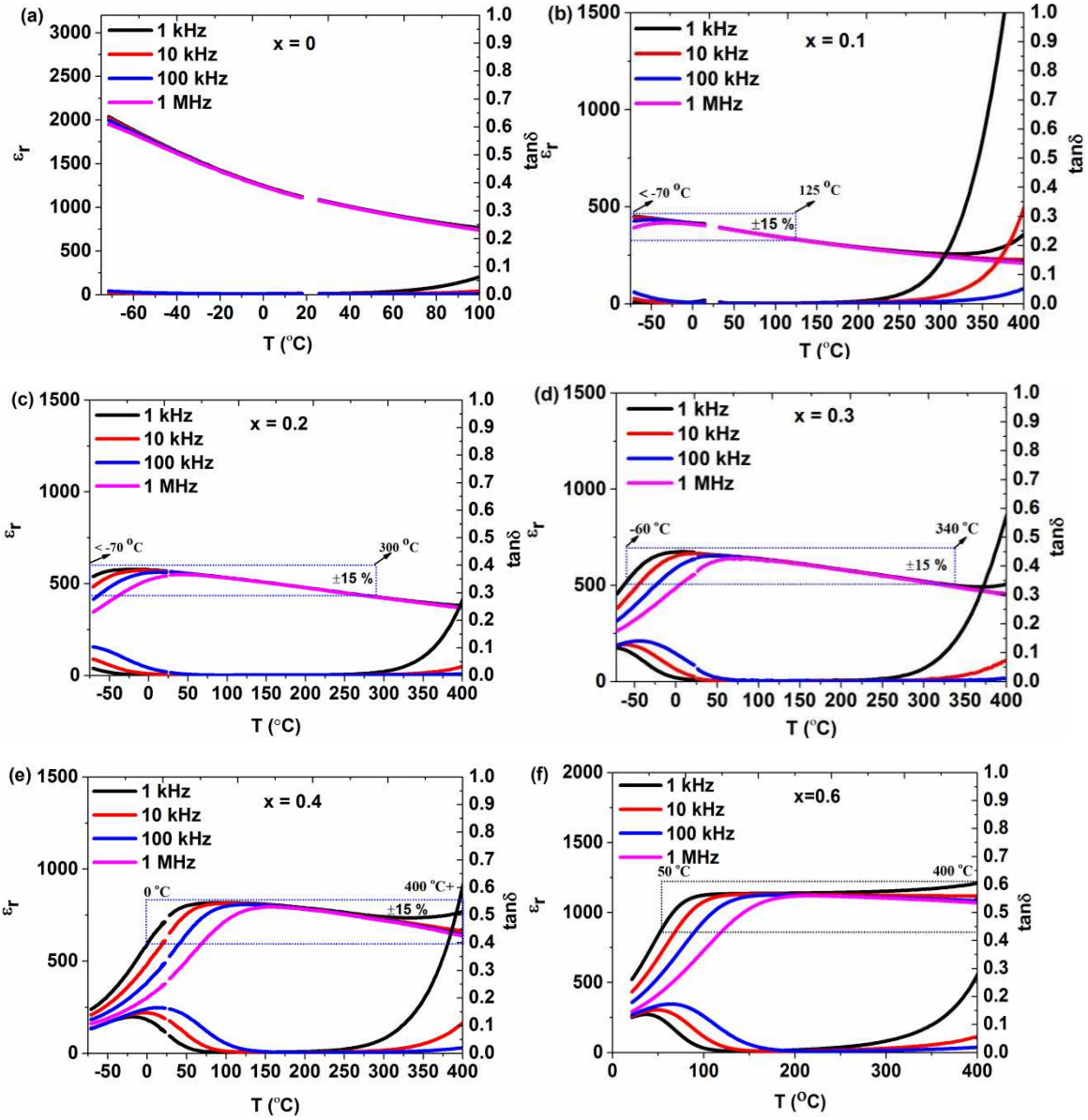

Figure 3. Relative permittivity, ε_r, and loss tangent, tanδ, versus temperature for (1-x)$Ba_{0.6}Sr_{0.4}Zr_{0.2}Ti_{0.8}O_3$ - x$Bi(Mg_{0.5}Ti_{0.5})O_3$: (a) x = 0; (b) x = 0.1; (c) x = 0.2; (d) x = 0.3 (e) x=0.4 and (f) x=0.6. Breaks in plots represent changeover between low and high temperature measurement equipment.

Table 1. Summary of the dielectric properties (at 1 kHz), resistivity and RC constant for (1-x)$Ba_{0.6}Sr_{0.4}Zr_{0.2}Ti_{0.8}O_3$ - x$Bi(Mg_{0.5}Ti_{0.5})O_3$ system.

Sample	ε_r/25ºC	T_m/ºC	$\varepsilon_{r\ max}$	$\varepsilon_{r\ mid}$±15% T-range (1 kHz)	tanδ ≤ 0.02, 1 kHz (T-range)	Resistivity, ρ(Ω.m) at 300 ºC	RC constant (s) at 300 ºC
x = 0	1090	-	-	-	-70 ºC–70 ºC	~10^{10}	-
x= 0.1	400	-70	450	<-70 ºC-125 ºC (400 ± 15%)	-70 ºC-230 ºC	-	-
x= 0.2	**560**	**-20**	**580**	**<-70 ºC-300 ºC (500 ± 15%)**	**-60 ºC-310 ºC**	**~10^9**	**3.7**
x=0.3	670	10	670	-60 ºC-340 ºC (590 ± 15%)	-10 ºC-280 ºC	-	-
x=0.4	750	80	820	0 ºC-400 ºC + (710 ± 15%)	50 ºC-270 ºC	~ 10^9	6.5
x =0.6	560	110	1140	50 ºC-400 ºC (990 ± 15%)	100 ºC-250 ºC	-	-

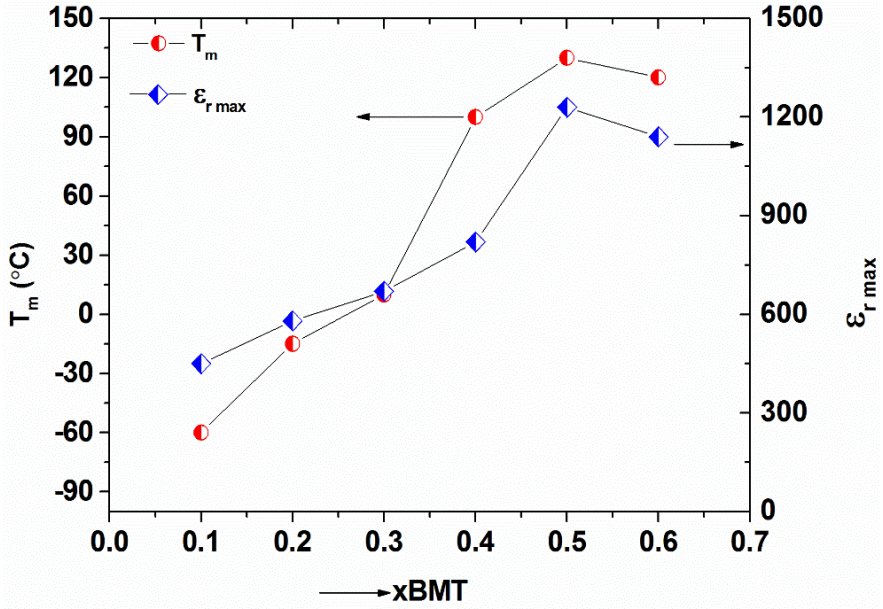

Figure 4. Maximum relative permittivity (1 kHz) and its corresponding temperature (T_m) as a function of composition x in (1-x)$Ba_{0.6}Sr_{0.4}Zr_{0.2}Ti_{0.8}O_3$ – x$Bi(Mg_{0.5}Ti_{0.5})O_3$: x = 0.1 – 0.6.

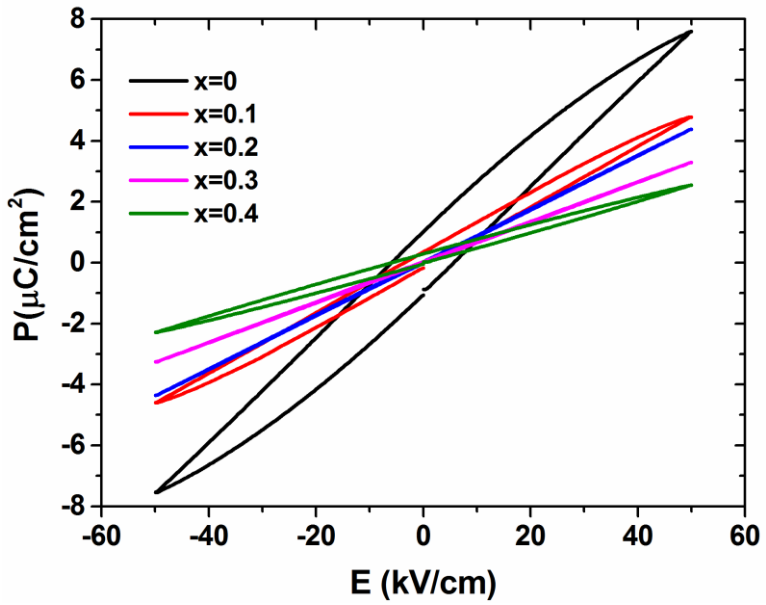

Figure 5. Polarisation-electric field response for (1-x)$Ba_{0.6}Sr_{0.4}Zr_{0.2}Ti_{0.8}O_3$ – x$Bi(Mg_{0.5}Ti_{0.5})O_3$.

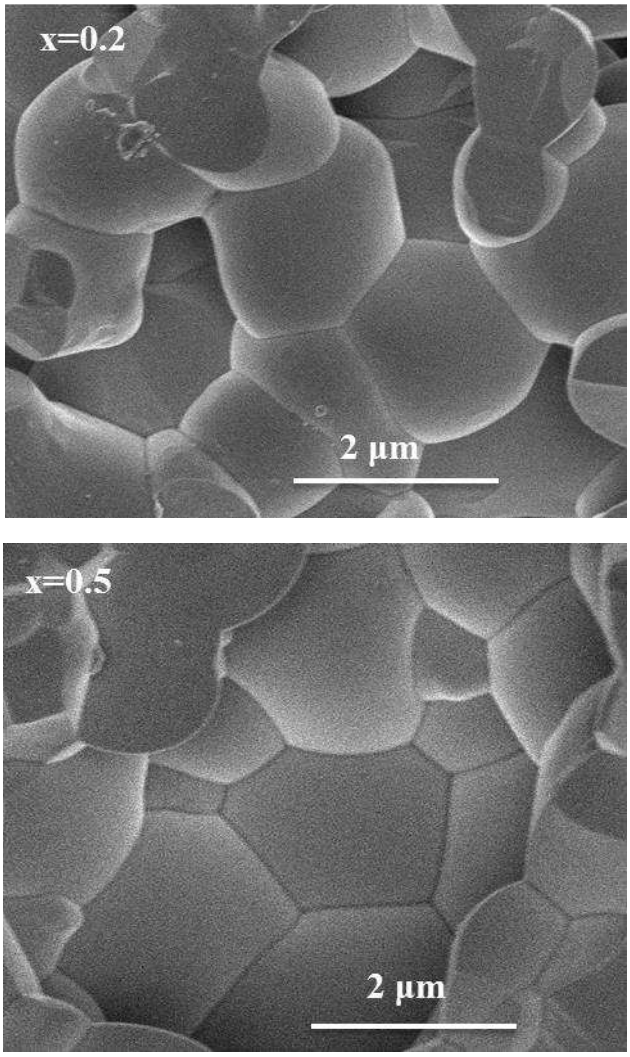

Figure 6. SEM micrographs of (1-x)$Ba_{0.6}Sr_{0.4}Zr_{0.2}Ti_{0.8}O_3$ – x$Bi(Mg_{0.5}Ti_{0.5})O_3$, x = 0.2 and x = 0.5.

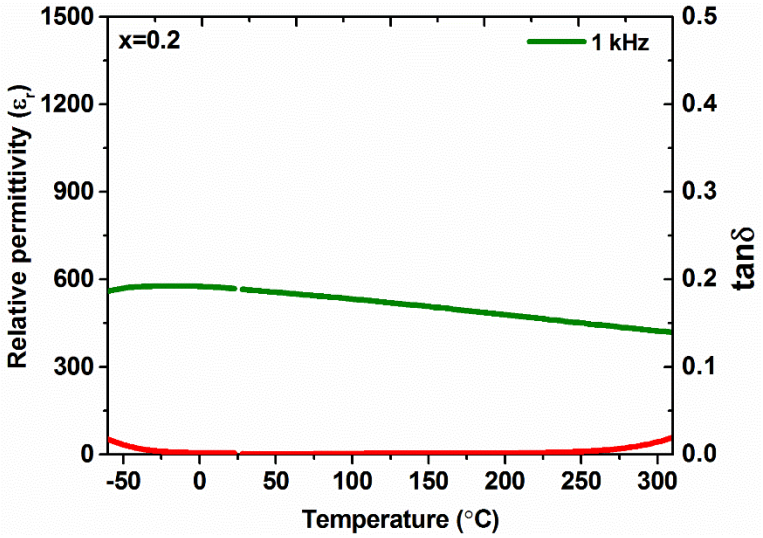

Figure 7. Relative permittivity, ε_r, and loss tangent, tanδ, versus temperature at a single frequency, 1 kHz, for sample composition x = 0.2 in the system (1-x)$Ba_{0.6}Sr_{0.4}Zr_{0.2}Ti_{0.8}O_3$ – x$Bi(Mg_{0.5}Ti_{0.5})O_3$.

for PbO volatilisation) [22-27]. Future refinements to high-temperature ceramic processing conditions may reduce lattice defects and associated conduction processes.

Polarisation-electric measurements for x = 0 yielded a slim P-E loop with some non-linearity. However, samples x ≥ 0.1 gave a polarisation–electric field responses consistent with a very low loss capacitor material, Figure 5.

The relative densities of the ceramics were estimated to be ≥ 90 % of theoretical density: grain sizes were < 3 μm, Figure 6.

The properties of x = 0.2 compare very favourably with other high temperature dielectric ceramics that have been discovered in recent years in the search for new and improved capacitor materials. From an applications perspective, it is important that stable dielectric permittivity is accompanied by low dielectric losses. The new (1–x)BSZT–xBMT material, x = 0.2, achieves this, exhibiting tanδ ≤ 0.015 across the full target temperature range from -55 °C to 300 °C (1 kHz). A number of publications in the literature fail to emphasis the temperature range of both stable permittivity and low dielectric loss, the temperature range of stable permittivity is often highlighted without giving equal weight to the temperature range of low tanδ - which is usually more restricted in temperature range. The 1 kHz response of x = 0.2 is plotted in Figure 7 to highlight its very promising temperature stabile dielectric properties.

The dielectric losses in $0.8Ba_{0.6}Sr_{0.4}Zr_{0.2}Ti_{0.8}O_3 – 0.2Bi(Mg_{0.5}Ti_{0.5})O_3$ are lower than for alternative temperature-stable materials with similar levels of stability in $\varepsilon_r(T)$ and similar $\varepsilon_{r\ mid}$ values ~ 500, for example, $(Ba,Ca)TiO_3$-$Bi(Mg_{0.5}Ti_{0.5})O_3 – NaNbO_3$ [1, 8]. One reason for this is the very low T_m value in $0.8Ba_{0.6}Sr_{0.4}Zr_{0.2}Ti_{0.8}O_3 – 0.2Bi(Mg_{0.5}Ti_{0.5})O_3$. Consequently the tanδ relaxor dispersion peak (1 kHz) is displaced to well below -55 °C (Figure 3) and this avoids any significant increase in tanδ as temperature cools to -55 °C.

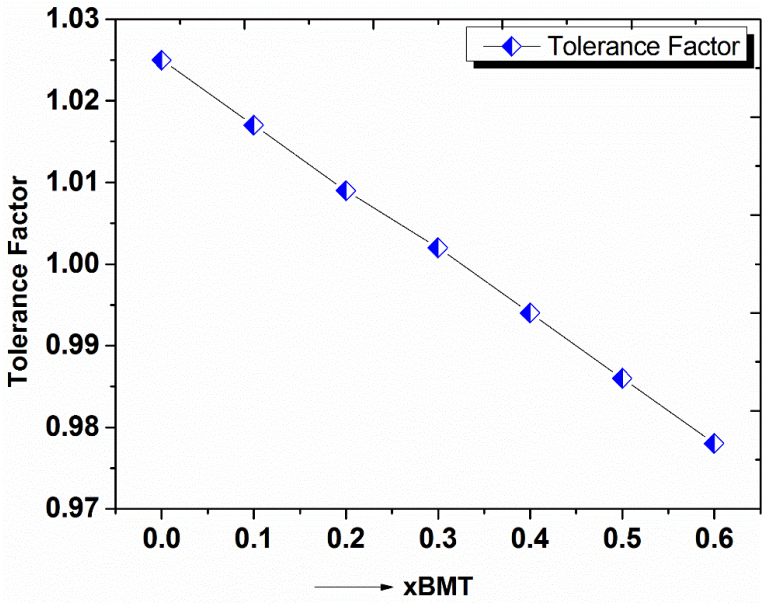

Figure 8. Goldschmidt tolerance factors for (1-x)$Ba_{0.6}Sr_{0.4}Zr_{0.2}Ti_{0.8}O_3$ – x$Bi(Mg_{0.5}Ti_{0.5})O_3$.

The Goldschmidt tolerance factors are plotted in Figure 8, values were calculated based on Shannon ionic radii where available, but there is uncertainty in the Bi^{3+} radii; in common with recent publications an estimated value of 1.36 Å was used. There was an opposed trend in tolerance factor and T_m values(Figures 4 and 8) but the significance of this is uncertain. In common with other temperature stable relaxors, the present materials incorporate Bi^{3+} on the perovskite lattice. The importance of A-site Bi^{3+} in supressing the normal rise in permittivity on cooling below the Burn's temperature, and imparting temperature stable properties is presumed to relate to a changing polar nanostructure arising from the characteristics of the electronic structure and orbital/bonding energies of Bi^{3+}. Hybridisation of 6s and 6p orbitals, asymmetry in Bi-O bond lengths and Bi displacements from the standard lattice position are discussed in standard crystallographic texts [27 It is noted that the optimum composition, x = 0.2, has a 20 % B site occupancy of Bi ions, much lower than the 50 % average occupancy in the best temperature-stable composition in the related (1-x)$Ba_{0.8}Ca_{0.2}TiO_3$- x$Bi(Mg_{0.5}Ti_{0.5})O_3$ system. Moreover, the x = 0.5 composition in the latter has a 25% Mg occupancy of B-sites, as opposed to 10 % for the optimum 0.8$Ba_{0.6}Sr_{0.4}Zr_{0.2}Ti_{0.8}O_3$ – 0.2$Bi(Mg_{0.5}Ti_{0.5})O_3$ composition, indicating that co-substitution with Zr is also important in supressing the normal relaxor behaviour (at T > Tm). Off-valent Mg^{2+} and isovalent Zr^{4+} substituents on Ti^{4+} sites are each 'inactive' ions (non-displaced in BO_6 octahedra) and they aqre expected, along with Bi^{3+} on A sites, to play a role in supressing the normal rise in polarisation in the ergodic relaxor region. However, the detailed reasons why Bi^{3+} A- site substitution and concomitant B-site substitution supress the normal relaxor peak are not understood at this stage. A full mechanistic understanding requires future analysis of local structure supported by atomistic modelling [28].

Conclusions

In the search for temperature-stable dielectrics with extended operating range, as required for future capacitor applications, very promising properties have been demonstrated in the novel perovskite solid solution system: (1–x)$Ba_{0.6}Sr_{0.4}Zr_{0.2}Ti_{0.8}O_3$ – x$Bi(Mg_{0.5}Ti_{0.5})O_3$. Composition x = 0.2 exhibits stable relative permittivity, ε_r = 500 ± 15 % (1 kHz) with low dielectric loss, tanδ ≤ 0.02 (1 kHz) across the temperature range, -55 to 300 °C. A linear polarisation–electric field response (50 kV, 1 Hz) is also promising and suggest the material is worthy of further development as a potential high temperature dielectric material. The mechanisms conferring temperature

stability across extremes of temperature are thought to relate to the bonding characteristics of Bi^{3+} ions A-sites, as well as 'inactive' Zr and Mg ions on B-sites of the perovskite ABO_3 crystal lattice.

Acknowledgements

Saeed ullah Jan and Aurang Zeb are thankful to the Higher Education Commission (HEC) Government of Pakistan and Islamia College Peshawar Khyber Pukhoon khawa (KPK) for financial support. Authors wish to thank colleagues and collaborators for useful discussions.

References:

1. Zeb A, Bai Y, Button T, and Milne SJ, "Temperature-Stable Relative Permittivity from− 70° C to 500° C in ($Ba_{0.8}Ca_{0.2}$) TiO_3–$Bi(Mg_{0.5}Ti_{0.5})O_3$–$NaNbO_3$ Ceramics", J. Am. Ceram. Soc., **97**[8] 2479-83 (2014).
2. Dittmer R, Anton EM, Jo W, Simons H, Daniels JE, Hoffman M, Pokorny J, Reaney IM, and Rödel J, "A High-Temperature-Capacitor Dielectric Based on $K_{0.5}Na_{0.5}NbO_3$-Modified $Bi_{1/2}Na_{1/2}TiO_3$–$Bi_{1/2}K_{1/2}TiO_3$," J. Am. Ceram. Soc., **95**[11] 3519-24 (2012).
3. Zeb A and Milne SJ, "Stability of High-Temperature Dielectric Properties for (1−x) $Ba_{0.8}Ca_{0.2}TiO_3$–x$Bi(Mg_{0.5}Ti_{0.5})O_3$ Ceramics," J. Am. Ceram. Soc., **96**[9] 2887-92 (2013).
4. Xiong B, Hao H, Zhang S, Liu H, and Cao M, "Structure, dielectric properties and temperature stability of $BaTiO_3$–$Bi(Mg_{1/2}Ti_{1/2})O_3$ perovskite solid solutions," J. Am. Ceram. Soc., **94**[10] 3412-17 (2011).
5. Zhang Q, Li Z, Li F, Xu Z, "Structural and Dielectric Properties of $BaTiO_3$–$Bi(Mg_{0.5}Ti_{0.5})O_3$ Lead-Free Ceramics," J. Am. Ceram. Soc.,**94**[12]: 4335–39(2011).
6. Choi DH, Baker A, Lanagan M, Trolier-McKinstry S, and Randall C, "Structural and Dielectric Properties in (1-x)$BaTiO_3$–x$Bi(Mg_{1/2}Ti_{1/2})O_3$ Ceramics ($0.1 \leq x \leq 0.5$) and Potential for High-Voltage Multilayer Capacitors," J. Am. Ceram. Soc., **96**[7] 2197-2202 (2013).
7. Wada, S., Yamato, K., Pulpan, P., Kumada, N., Lee, B.-Y., Iijima, T., Moriyoshi, C. and Kuroiwa, Y. "Piezoelectric properties of high Curie temperature barium titanate–bismuth perovskite-type oxide system ceramics", J. Appl. Phys., **108[**9]. 094114 (2010).
8. Zeb A and Milne SJ, "Dielectric Properties of $Ba_{0.8}Ca_{0.2}TiO_3$–$Bi(Mg_{0.5},Ti_{0.5})O_3$–$NaNbO_3$ Ceramics," J. Am. Ceram. Soc., **96[**12] 3701-3703 (2013).
9. Zeb A and Milne SJ, Temperature-stable dielectric properties from -20 °C to 430 °C in the system $BaTiO_3$–$Bi(Mg_{0.5}Z_{0.5})O_3$, Journal of the European Ceramic Society, **34**[13] 3159-66 (2014).
10. Raengthon N, Sebastian T, Cumming D, Reaney IM, and Cann DP, "$BaTiO_3$–Bi ($Zn_{1/2}Ti_{1/2}$) O_3–$BiScO_3$ Ceramics for High-Temperature Capacitor Applications," Journal of the American Ceramic Society, **95**[11] 3554-61 (2012).
11. Dittmer R, Jo W, Damjanovic D, and Rödel J, "Lead-free high-temperature dielectrics with wide operational range," Journal of Applied Physics, **109**[3] 034107-07-5 (2011).
12. Zeb A and Milne SJ, "Low variation in relative permittivity over the temperature range 25–450° C for ceramics in the system (1-x)[$Ba_{0.8}Ca_{0.2}TiO_3$]–x[$Bi(Zn_{0.5}Ti_{0.5})O_3$]. J. Eur. Ceram Soc., **34** 3159-3166 (2014).
13. Zhu F, Skidmore TA, Bell AJ, Comyn TP, James C, Ward M, and Milne SJ, Diffuse dielectric behaviour in $Na_{0.5}K_{0.5}NbO_3$–$LiTaO_3$–$BiScO_3$ lead-free ceramics, Materials Chemistry and Physics, **129**[1] 411-17 (2011).
14. Skidmore TA, Comyn TP and Milne SJ, "Dielectric and piezoelectric properties in the system :(1−x)[$(Na_{0.5}K_{0.5}NbO_3)_{0.93}$–$(LiTaO_3)_{0.07}$]–x[$BiScO_3$]. J. Am. Ceram. Soc., 93[3] 624-626 (2010).

15. Zeb A and Milne SJ, "Dielectric and Piezoelectric Properties of (1-x) $K_{0.5}Bi_{0.5}TiO_3$–$xBa(Ti_{0.8}Zr_{0.2})O_3$ Ceramics," J. Am. Ceram. Soc., **96**[10] 3089-93 (2013).
16. Lim JB, Zhang S, Kim N, and Shrout TR, "High-Temperature Dielectrics in the $BiScO_3$–$BaTiO_3$–$(K_{1/2}Bi_{1/2})TiO_3$ Ternary System," J. Am. Ceram. Soc., **92**[3] 679-82 (2009).
17. Kruea-In C, Rujijanagul G, Zhu FY, and Milne SJ, "Relaxor behaviour of $K_{0.5}Bi_{0.5}TiO_3$-$BiScO_3$ ceramics," Appl. Phys. Lett., **100**[20] 202904 (2012).
18. Shi J, Fan HQ, Liu X, Ma Y and Li Q, Bi Deficiencies Induce High Permittivity in Lead-free BNBT-BST high-temperature dielectrics. J Alloys Compounds, **627**, 463-467 (2015).
19. Zhang N, Li L, Chen J and Yu J, ZnO-doped $BaTiO_3$-$Na_{0.5}Bi_{0.5}TiO_3$-Nb_2O_5 based ceramics with temperature-stable high permittivity from -55 to 375 °C, Mats. Letts., 138, 228-230 (2015).
20. Acosta M, Zang J, Jo W and Rödel J, "High-temperature dielectrics in $CaZrO_3$-modified $Bi_{1/2}Na_{1/2}TiO_3$-based lead-free ceramics. J. Eur. Ceram. Soc., **32**[16], 4327-4334 (2012).
21. Zeb A and Milne SJ, 'High temperature dielectric ceramics: a review of temperature-stable high-permittivity perovskites' J Mater Sci: Mater Electron, 26 [12]; 9243-9255.
22. Milne SJ and West AR, Compound Formation and Conductivity in the System Na_2O-ZrO_2-P_2O_5 – Sodium Zirconium Orthophosphates Solid State Ionics **9-10**: 865-868 (1983).
23. Milne SJ and West AR, Zr-Doped Na_3PO_4 – Crystal Chemistry- Phase Relations and Polymorphism Solid State Chem **57(**2): 166-177 (1985).
24. Milne SJ and West AR, Conductivity of Zr-Doped Na_3PO_4 – a new Na^+ ion Conductor Mats Res Bull., **19** [6] 705-710 (1984)
25. Bongkarn T, Rujijanagul G, and Milne SJ, Effect of excess PbO on phase formation and properties of $(Pb_{0.9}Ba_{0.1})ZrO_3$ ceramics. Materials Letters, **59**(10), pp.1200-1205 (2005).
26. Bongkarn T, Rujijanagul G and Milne SJ, Antiferroelectric-ferroelectric phase transitions in $Pb_{1-x}Ba_x\,ZrO_3$ ceramics: Effect of PbO content. Appl. Phys. Lett., **92**(9), p.092905 (2008).
27. Zeb A, Hall DA, Milne SJ, Lead-free piezoelectric $K_{0.5}Bi_{0.5}TiO_3$–$Bi(Mg_{0.5}Ti_{0.5})O_3$ ceramics with depolarisation temperatures up to ~220 ºC, J Mater Sci: Mater Electron, 26 [12]; 9512-9516.
28. Goodenough JB and Longo M, Landolt-Börnstein In - Group III Condensed Matter Vol. 4a pp 144-144 (1970) DOI: 10.1007/10201420_46.
29. Krayzman V, Levin I, Woicik JC and Bridges F, Correlated rattling-ion origins of dielectric properties in re-entrant dipole glasses $BaTiO_3$-$BiScO_3$, Appl. Phys. Letts **107**, 192903 (2015); DOI: 10.1063/1.4935417.